DEM SIMULATIONS OF QUASI-STATIC SHEAR DEFORMATION OF GRANULAR MEDIA

COLIN THORNTON

Civil & Mechanical Engineering Division
School of Engineering & Applied Science
Aston University
Aston Triangle, Birmingham B4 7ET, UK

Abstract: Results are presented of numerically simulated three dimensional quasi-static shear deformation of polydisperse systems of spheres. Results of axisymmetric compression test simulations are reported for both dense and loose systems. The versatility of numerical simulation is demonstrated by presenting results obtained from simulations of general radial deviatoric loading, a constant deviatoric strain test and a multi-axial plane strain test. In all cases, the simulated stress-strain dilation responses are in excellent qualitative agreement with the behaviour of granular materials observed in physical experiments.

1. Introduction

The Distinct (or Discrete) Element Method developed by Cundall and Strack [1] was originally intended as a research tool for the investigation of the micromechanics of granular materials in order to identify the appropriate physically sound continuum model which might then be incorporated into finite element analyses of engineering scale problems. Little progress has been made to achieving this long term goal. However, of more immediate benefit is the ability of DEM simulations to provide new information about what happens inside granular systems. Such information together with the facility to change the properties of the particles and conduct sensitivity studies, enhances our understanding of the physics of granular media and provides a rational framework for decision making. A further benefit of DEM simulations is that comparisons between sets of test data do not suffer from the inability to create exact replicates of the physical system, which is an inherent problem in laboratory studies.

Most of the early DEM applications were restricted to 2D assemblies of discs, Cundall and Strack [2], Thornton and Barnes [3], Rothenburg and Bathurst [4]. Due to the kinematic constraints on particle movements in 2D and the limited loading paths available, comparisons with real experiments in the 3D world were always ambiguous. Following the development of the 3D simulation code TRUBAL, Cundall [5], it is possible to explore the ability of the Discrete Element Method to simulate quasi-static shear deformation of granular media under general 3D states of stress and to compare the results obtained, at least qualitatively, with laboratory

experiments performed in true triaxial apparatuses. In the paper, we present results of numerical simulations of three-dimensional polydisperse systems of elastic spheres subjected to radial deviatoric loading, constant deviatoric strain and multi-axial plane strain.

In developing constitutive equations to model granular media as a continuum, the tradition has been to check the ability of the mathematical models to predict the observed behaviour in real experiments. However, the need to model complex 3D loading histories requires experiments to be carried out using the so-called "true triaxial apparatuses". These modern testing devices are extremely complicated and the reliability of the data obtained is still uncertain. If the experimentalist checks the constitutive modeller, who checks the experimentalist? It is simpler to devise algorithms which will enable appropriate DEM simulations to be performed using a periodic cell rather than to execute the same tests on laboratory specimens. In order to demonstrate that DEM simulated output data compares favourably with results from physical experiments, the results presented in the paper are restricted to observations regarding the macroscopic behaviour. Sources of information about the evolution of internal variables associated with the micromechanics and physics at the grain scale are indicated in the text.

2. Simulation Details

The Aston version of the TRUBAL code used for the numerical simulations reported here models the particles as elastic spheres with interparticle friction and adhesion. The interactions between contiguous particles are simulated by algorithms which are based on theoretical contact mechanics, Thornton and Yin [6]. For information about the numerical methodology the reader is referred to Cundall and Strack [1], Barnes [7] and Cundall [5]. In three dimensions, tests are simulated on a representative volume element, with periodic boundaries, subjected to uniform strain fields [5]. In this way "perfect" experiments are obtained free from boundary effects. The ensemble average stress tensor and moduli are calculated according to statistical mechanics formulations, Thornton and Barnes [3], Thornton [8].

The simulation program models the particle interactions as a dynamic process and the time evolution of the system is advanced using a simple explicit finite difference scheme. Application of the code involves cyclic calculations. At any time t, interparticle force increments are calculated at all contacts from the relative velocities of the contacting particles using incremental force-displacement rules. The interparticle forces are updated and, from the new out-of-balance force and moment on each particle, new particle accelerations (both linear and rotational) are obtained using Newton's second law. Numerical integration of the accelerations, using a small timestep Δt, provides new particle velocities which are then numerically integrated to give displacement increments from which the new particle positions are obtained. Having obtained new positions and velocities for all the particles, the program repeats the cycle of updating contact forces and particle locations. Checks are incorporated to identify new contacts and contacts that no longer exist.

Results are presented for a system of 3620 spheres which are modelled as elastic with interface friction and adhesion. Five different sizes of spheres were used, the smallest diameter was 0.135 mm, the largest was 0.4 mm and the average particle diameter was 0.26 mm. All the particles were attributed with the following properties: Young's modulus $E = 70$ GPa, Poisson's ratio $\nu = 0.3$ and notional solid density $\rho = 2650$ kg/m^3. The timestep used in the simulations is based on the minimum particle size and the Rayleigh wave speed, Thornton and Randall [9]. Consequently, for particles of diameter ca. 1 mm the timestep would be ca. 1 μs and, in order to ensure quasi-static deformation by using a strain rate of not more than 10^{-5} s^{-1}, it would require 10^{10} timesteps to apply 10% strain. Therefore, to complete the simulations within a reasonable timescale, the notional particle density is scaled up by a factor of 10^{12} in order to use a timestep ca. 1 μs. As a consequence, the forces and displacements, and hence the stresses and strains, are not affected; the velocities and accelerations are reduced by the implied inertial damping but these are not of concern when considering quasi-static behaviour.

The spheres were randomly generated within a cuboidal periodic cell of dimension 4.3 mm to provide an initial assembly with a solid fraction ca. 0.5 and no interparticle contacts. After generation, the assembly was subjected to isotropic compression using a strain rate of 10^{-4} s^{-1}. During simulation of isotropic compression servo-control algorithms were periodically introduced to maintain a desired stress level until the solid fraction and coordination number had attained constant values and a quasi-equilibrium state had been achieved. In order to create a dense system for subsequent shear simulations, the interparticle friction was set to zero during the isotropic compression stage. To prepare a loose system, isotropic compression was simulated with $\mu = 0.3$. In both cases, the interparticle friction and interface energy were adjusted to the desired values prior to shearing. During the shear stage simulations, a strain rate of 10^{-5} s^{-1} was employed and the particles were attributed with a coefficient of interparticle friction $\mu = 0.3$ and interface energy of adhesion $\Gamma = 0.6$ J/m^2, except when investigating the effect of varying friction on the system response.

Isotropically compressed specimens were prepared for subsequent shear deformation at a constant mean stress of 100 kPa. At the start of the shear stage the solid fraction of the dense system was 0.660 and that of the loose system was 0.618. At the end of isotropic compression the average coordination numbers were 6.07 and 5.02 for the dense and loose systems respectively.

3. Axisymetric Compression

Simulations of axisymmetric compression, $\sigma_1 > \sigma_2 = \sigma_3$, were performed in which servo-control algorithms were used to maintain a constant mean stress, $p = (\sigma_1 + \sigma_2 + \sigma_3) / 3 = 100$ kPa. Figure 1 shows the evolution of the deviator stress $(\sigma_1 - \sigma_3)$ with deviator strain $(\varepsilon_1 - \varepsilon_3)$ for both the dense and loose systems. The initial shear modulus is much higher for the dense system which exhibits a peak in the stress strain curve at about 5% strain followed by strain softening behaviour.

The loose system does not exhibit any strain softening, the deviator stress increases at a decreasing rate until an essentially constant value is reached at about 15% strain. It is noted that the stress-strain response of the dense system demonstrates that strain softening is a genuine material behaviour and not necessarily the result of non-uniform deformation due to the existence of platen boundaries, which can be the case in laboratory experiments.

The corresponding evolution of the void ratio in the two tests is shown in Figure 2. The changes in void ratio show that the dense system expands and the loose system contracts. At large strains, both systems deform at constant volume and this is associated with a constant deviator stress which is independent of the initial void ratio. From traditional soil mechanics, we would expect that the constant volume deformation at large strains is associated with a "critical void ratio" which is independent of the initial void ratio. The figure shows that, at 30% deviator strain, the void ratio is not exactly the same for the two systems: 0.598 for the dense

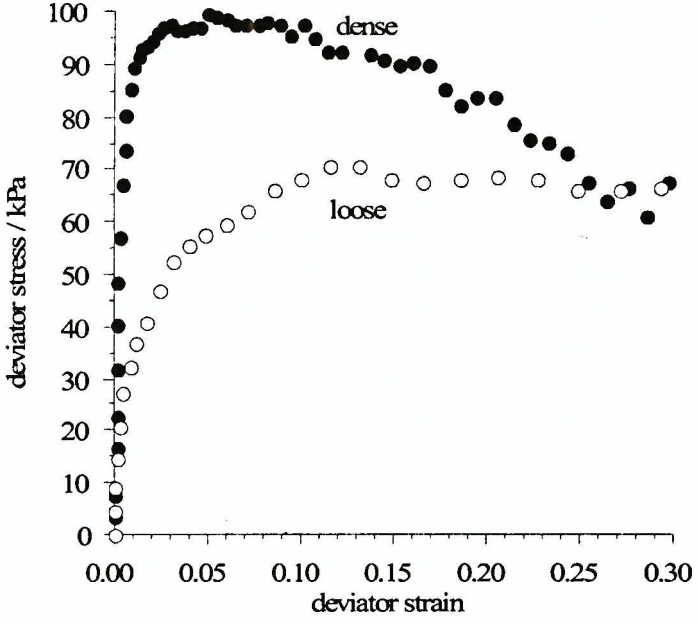

Figure 1. Axisymmetric compression stress-strain curves

system, 0.606 for the loose system. However, in recently completed simulations on polydisperse systems of 8000 spheres (not reported here) it has been found that the critical void ratio is attained at approximately 50% axial strain.

The above figures show that, qualitatively, the stress-strain-dilation response obtained for both the dense and loose systems is typical of that obtained in laboratory experiments. Further axisymmetric compression simulations have been performed on the dense system, Thornton and Sun [10], in which repeated unload-reload cycles were applied under both constant stress amplitude and constant strain

amplitude conditions. For large amplitude cyclic loading in which the system was repeatedly switched between axisymmetric compression and axisymmetric

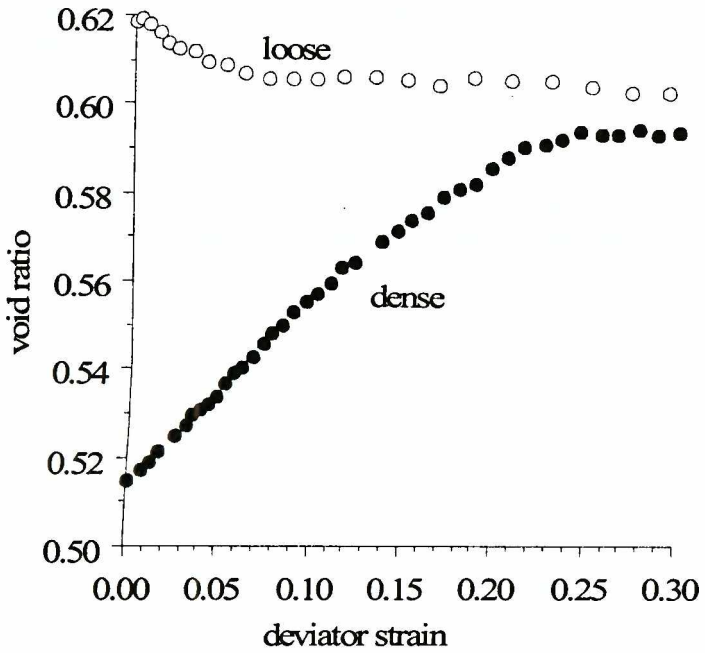

Figure 2. *Evolution of void ratio during axisymmetric compression*

extension, the simulated volumetric strain evolution exhibited the so-called "butterfly shape" observed in laboratory experiments. The macroscopic behaviour illustrated in Figures. 1 and 2 in some way relates to the micromechanics and physics occurring at the grain scale. Details of the corresponding evolution of the induced structural anisotropy, the percentage of sliding contacts, the average coordination number, distribution of the magnitude of the contact forces and how they contribute to the state of stress are provided by Thornton [11], Thornton and Antony [12].

Effect of interparticle friction

In real experiments it is difficult to distinguish between the effects of contact friction and particle shape. Numerical simulations allow the effects of contact friction to be isolated. Thornton and Sun [13] reported simulations of axisymmetric compression using two different coefficients of interparticle friction of $\mu = 0.3$ and $\mu = 0.6$ specified for both the dense and loose systems, with no interparticle adhesion. The results showed that an increase in the interparticle friction resulted in an increase in shear modulus and shear strength for both systems. Details of the effect of interparticle friction on the micromechanics of granular media are provided by Thornton [11].

Further axisymmetric compression test simulations have been performed on the dense system at a constant mean stress of 100 kPa with a different value of μ

specified for each test, Thornton [11]. Figure 3 illustrates the effect of interparticle friction on the mobilised shear strength defined in terms of the so-called angle of internal friction φ, where $\sin \varphi = (\sigma_1 - \sigma_3) / (\sigma_1 + \sigma_3)$. Two sets of data obtained from the simulations are shown, corresponding to the peak value $\sin \varphi_{max}$ and the value at the critical state $\sin \varphi_{cv}$, together with experimental measurements of $\sin \varphi_{cv}$ reported by Skinner [14]. There is reasonable agreement between the simulated and experimental data except when the coefficient of interparticle friction approaches zero. Skinner's [14] data suggests that $\sin \varphi_{cv}$ is independent of interparticle friction but the results of the simulations are more convincing since random assemblies of frictionless spheres are unstable at all of the contacts all of the time; making it very

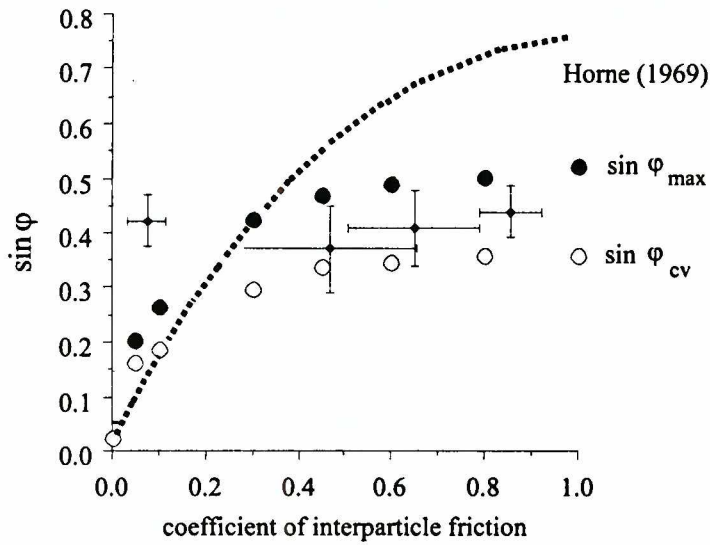

Figure 3. *Effect of interparticle friction on shear strength*

difficult to develop any stable force transmission through the system which would lead to the development of a deviator stress. The simulation carried out with $\mu = 0$ was difficult to execute and the corresponding data point shown on the figure is simply an average value obtained from the continuously fluctuating calculated deviator stress. In other words, we expect a system of frictionless spheres to behave like a liquid in that it offers no resistance to shear.

Also superimposed on Figure 3 is the theoretical relationship between φ_{cv} and μ suggested by Horne [15]. The significant difference between the theoretical prediction and both simulated and experimental data arises from the fact that the theory ignores the possibility of particle rotation. Other simulations, not reported here, have demonstrated that if particle rotation is not permitted then the ensemble modulus and shear strength is significantly increased. Hence, we would expect that if particle rotation was inhibited then the simulation data may approach the theoretical curve.

4. Radial Deviatoric Loading

With the mean stress maintained at a constant value of 100 kPa, both dense and loose systems (for the case $\mu = 0.3$) were subjected to radial deviatoric loading paths in which the ratio

$$b = \frac{(\sigma_2 - \sigma_3)}{(\sigma_1 - \sigma_3)} \tag{1}$$

was maintained constant in each test, for the complete range $0 \le b \le 1$. In this way the deviatoric stress is monotonically increased along different radial stress paths on the Π-plane of principal stress space. The conventional axisymmetric compression test discussed in the previous section corresponds to $b = 0$ and $b = 1$ corresponds to axisymmetric extension. For each radial loading test simulation, the state of stress corresponding to failure was identified and plotted on the Π-plane, as illustrated in Figure 4. Superimposed on the figure is the failure criterion proposed by Lade and Duncan [16] which is defined by

$$\frac{I_1^3}{I_3} - 27 = \eta \tag{2}$$

where I_1 and I_3 are the first and third stress invariants respectively. The Lade and Duncan [16] failure criterion predicts that the strength (defined by $\sin \varphi_{max}$) in axisymmetric extension is greater than the strength in axisymmetric compression and this is confirmed by the numerical simulations. The simulation data, for both the dense and loose systems, do not support the criterion suggested by Matsuoka and Nakai [17] which predicts that the value of $\sin \varphi_{max}$ is the same in axisymmetric compression and axisymmetric extension. In the simulations it was observed that the maximum value of $\sin \varphi_{max}$ occurred when $b = 0.5$.

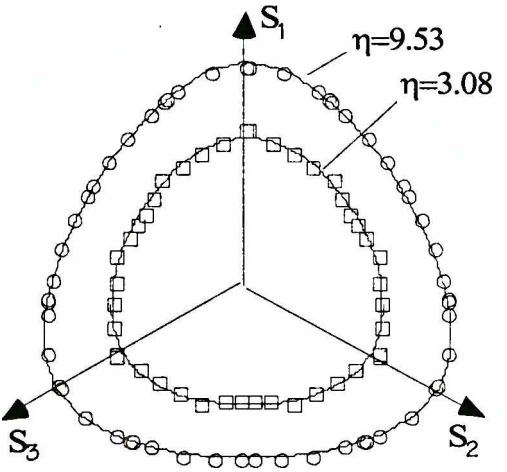

Figure 4. *Deviatoric failure states of stress, dense (○) loose (□)*

As observed in laboratory tests, Davoudzadeh [18], the stress-strain curves obtained depended on the direction of the radial loading path and various definitions of stress and strain were examined in an attempt to normalise the data sets. The best results are illustrated in Figure 5 in which the Lade and Duncan [16] parameter

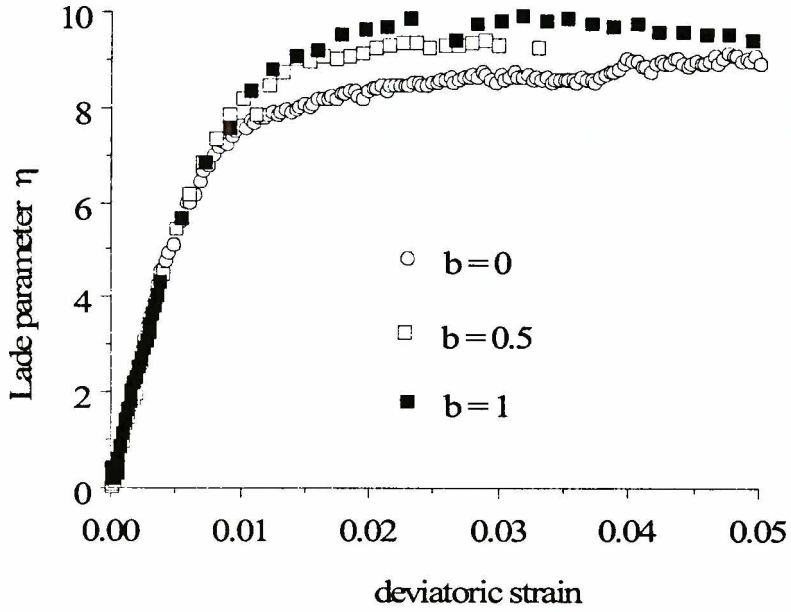

Figure 5. Evolution of η with deviatoric strain

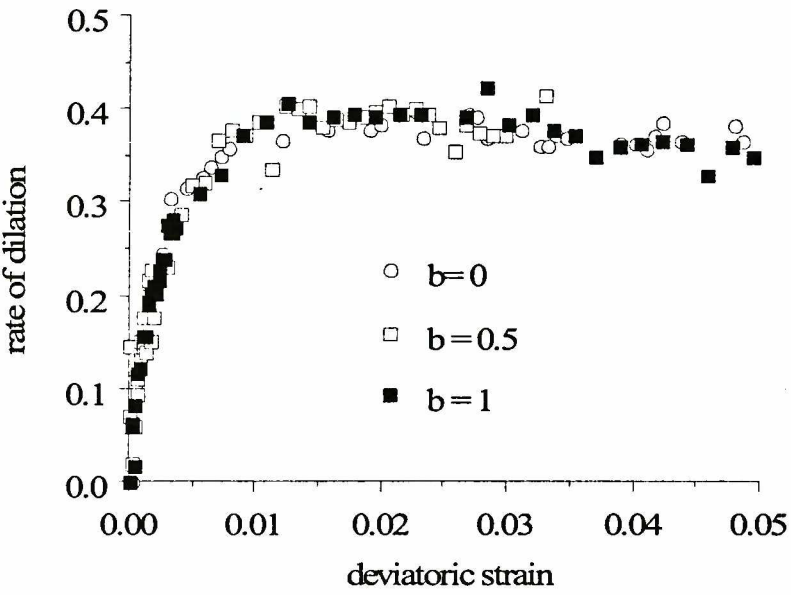

Figure 6. Evolution of rate of dilation with deviatoric strain

η is plotted against the deviatoric strain ε_d. For clarity, only the data obtained for $b = 0$, 0.5 and 1 are shown. The normalisation is very good for $\eta < 7$. Similar observations were made by Davoudzadeh [18] from laboratory tests on sand. It was also found from the numerical simulations that the evolution of the rate of dilation, defined by the ratio $(-d\varepsilon_v / d\varepsilon_d)$, was insensitive to the radial deviatoric loading path direction, as shown in Figure 6.

5. Non-Radial Deviatoric Loading

Figure 5 implies that if the deviatoric strain is maintained constant during shear then the stress state, as defined by the Lade and Duncan [16] parameter η, should not change. Therefore, a further test was simulated on the dense system. In this test, the system was subjected to a deviatoric strain of 0.285%, under axisymmetric

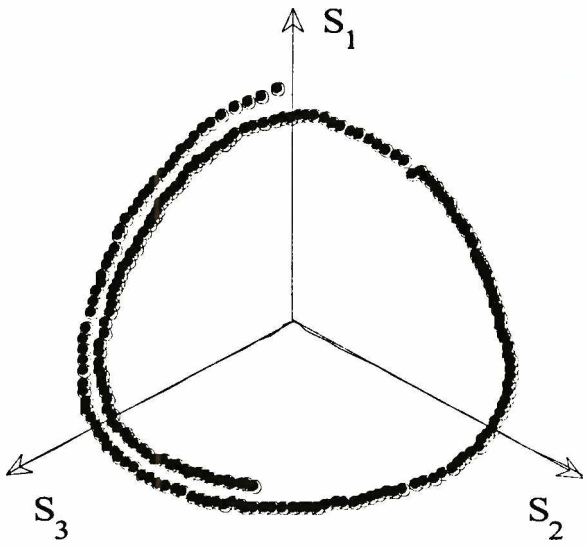

Figure 7. *Stress path evolution during constant deviatoric strain test*

compression conditions, which resulted in a mobilised deviatoric stress of 51.4 kPa. Then, a constant deviatoric strain test was simulated by designing servo-control algorithms to follow a circular strain path on the Π-plane of principal strain space. Throughout the test, the mean stress was maintained in the range 100±0.8 kPa. The resulting stress path followed on the Π-plane of principal stress space is shown in Figure 7 and it can be seen that, after a sudden initial drop in deviatoric stress, the stress path resembles in shape the geometry of the Lade and Duncan [16] failure surface.

Another example of non-radial deviatoric loading, which should not present significant technical problems in laboratory experiments using a true triaxial apparatus, is a multi-axial plane strain test. In this test the system was first of all subjected to axisymmetric compression until the deviatoric strain was 0.285% and the deviatoric stress was 51.4 kPa, as in the constant deviatoric strain test reported

above. Then, the strain state was gradually altered from axisymmetric compression to axisymmetric extension during which no strain was permitted in the 1-direction. When the axisymmetric extension state ($\varepsilon_{11}= \varepsilon_{22}$) was reached zero lateral strain was imposed in the 2-direction until the axisymmetric extension ($\varepsilon_{22}= \varepsilon_{33}$) state was attained and then zero lateral strain in the 3-direction was imposed until the axisymmetric extension ($\varepsilon_{11}= \varepsilon_{33}$) state was reached. Finally, with zero lateral strain in the 1-direction the system was returned to the initial axisymmetric compression ($\varepsilon_{22}= \varepsilon_{33}$) state. The resulting strain path on the Π-plane of principal strain space is triangular, Figure 8, which is traversed in a clockwise direction. A second test simulation following an anticlockwise strain path was also performed.

The corresponding stress paths on the Π-plane of principal stress space are shown in Figure 9. Initially, as the deviatoric strain vector rotates through 60° from an axisymmetric compression strain state to an axisymmetric extension state of strain, the corresponding deviatoric stress vector rotates through an angle of 79° tracing out a slightly curved stress path. Thereafter, the shape of the stress path

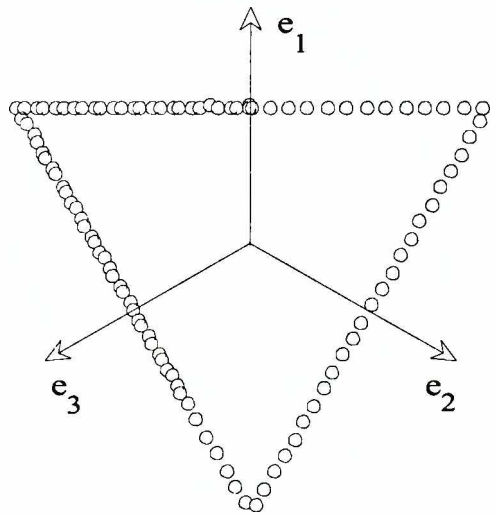

Figure 8. *Deviatoric strain path for multi-axial plane strain test*

followed is that of a curvilinear triangle with each apex occurring simultaneously with the corresponding apex on the triangular strain path.

Further details of the non-radial deviatoric loading simulations are provided by Thornton [11].

6. Concluding Remarks

Computer simulated experiments have been performed using a periodic cell subjected to a variety of uniform strain fields and the ensemble average stress tensor has been calculated according to statistical mechanics. The results presented in the paper show that qualitatively realistic macroscopic mechanical behaviour can be generated. However, the data can only be compared quantitatively with real

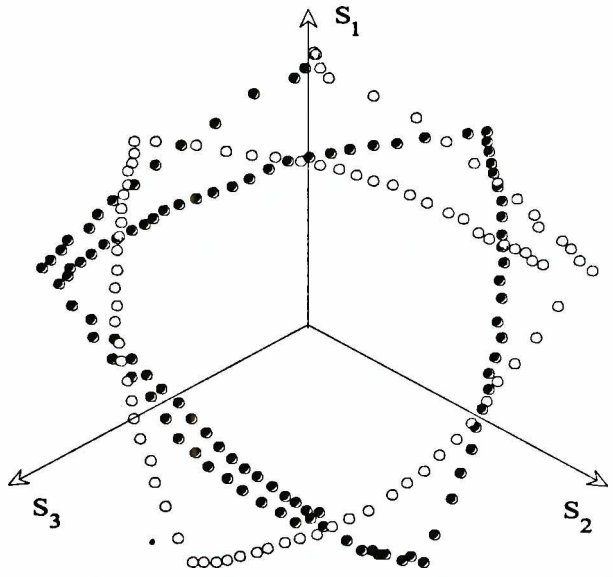

Figure 9. *Deviatoric stress paths for multi-axial plane strain test, clockwise rotation (○), anticlockwise rotation (●)*

experiments on materials such as glass ballotini. Particle shape is important and significantly affects the modulus, strength and dilation of granular media, as demonstrated in 2D simulations reported by Rothenburg and Bathurst [19].

References

[1] Cundall P. A., Strack O. D. L. (1979), *A discrete numerical model for granular assemblies*, Géotechnique 29, 47-65

[2] Cundall P. A., Strack O. D. L. (1983), *Modeling of microscopic mechanisms in granular materials*, In Mechanics of Granular Materials: New Models and Constitutive Relationships, Eds. J. T. Jenkins & M. Satake, pp. 137-149, Amsterdam: Elsevier

[3] Thornton C., Barnes D.J. (1986), *Computer simulated deformation of compact granular assemblies*, Acta Mechanica 64, 45-61

[4] Rothenburg L., Bathurst R. J. (1989), *An analytical study of induced anisotropy in idealised granular materials*, Géotechnique 39, 601-614

[5] Cundall P. A. (1988), *Computer simulations of dense sphere assemblies*, In Micromechanics of Granular Materials, Eds. M. Satake, J. T. Jenkins, pp. 113-123, Amsterdam: Elsevier

[6] Thornton C., Yin K. K. (1991), *Impact of elastic spheres with and without adhesion*, Powder Technology 65, 153-166

[7] Barnes D. J. (1985), *A study of the micro-mechanics of granular material*, PhD thesis, Aston University

[8] Thornton C. (1993), *On the relationship between the modulus of particulate media and the surface energy of the constituent particles*, J. Phys. D: Appl. Phys. 26, 1587-1591

[9] Thornton C., Randall C. W. (1988), *Applications of theoretical contact mechanics to solid particle system simulations*, In Micromechanics of Granular Materials, Eds. M. Satake & J. T. Jenkins, pp. 245-252, Amsterdam: Elsevier

[10] Thornton C., Sun G. (1994), *Numerical simulation of general 3D quasi-static shear deformation of particulate media*, In Numerical Methods in Geotechnical Engineering, Ed. I. M. Smith, pp. 143-148, Rotterdam: Balkema

[11] Thornton C. (1998), *Numerical simulations of deviatoric shear deformation of granular media*, (submitted for publication in Géotechnique)

[12] Thornton C., Antony S. J. (1998), *Quasi-static deformation of particulate media*, (submitted for publication in Phil. Trans. Roy. Soc. London A)

[13] Thornton C., Sun G. (1993), *Axisymmetric compression of 3D polydisperse systems of spheres*, In Powders & Grains 93, Ed. C. Thornton, pp. 129-134, Rotterdam: Balkema

[14] Skinner A. (1969), *A note on the influence of interparticle friction on the shearing strength of a random assembly of spherical particles*, Géotechnique 19, 150-157

[15] Horne M. R. (1969), *The behaviour of an assembly of rotund, rigid, cohesionless particles*, III. Proc. Roy. Soc. London A310, 21-34

[16] Lade P. V., Duncan J. M. (1975), *Elastoplastic stress-strain theory for cohesionless soil*, J. Geotech. Engng., Proc. ASCE, 101, 1037-1053

[17] Matsuoka H., Nakai T. (1974), *Stress-deformation relationship and strength characteristics of soil under three different principal stresses*, Proc. Japan Soc. Civ. Engrs. 232, 59-70

[18] Davoudzadeh F. (1982), *Responses of sand to three independently controlled principal stresses*, PhD thesis, London University (University College)

[19] Rothenburg L., Bathurst R. J. (1992), *Micromechanical features of granular assemblies with planar elliptical particles*, Géotechnique 42, 79-95